



Molecular Crystals and Liquid Crystals

Publication details, including instructions for authors and subscription information:

<http://www.tandfonline.com/loi/gmcl20>

Measuring and Monitoring Optically Induced Thermal or Orientational Non-Locality in Nematic Liquid Crystal

Marc Warengthem^a, Jean François Blach^a & Jean François Henninot^a

^a Laboratoire de Physico-Chimie des interfaces et Applications, LPCIA FRE CNRS, Université d'Artois, Lens cedex, France

Version of record first published: 22 Sep 2006

To cite this article: Marc Warengthem, Jean François Blach & Jean François Henninot (2006): Measuring and Monitoring Optically Induced Thermal or Orientational Non-Locality in Nematic Liquid Crystal, *Molecular Crystals and Liquid Crystals*, 454:1, 297/[699]-314/[716]

To link to this article: <http://dx.doi.org/10.1080/15421400600655881>

PLEASE SCROLL DOWN FOR ARTICLE

Full terms and conditions of use: <http://www.tandfonline.com/page/terms-and-conditions>

This article may be used for research, teaching, and private study purposes. Any substantial or systematic reproduction, redistribution, reselling, loan, sub-licensing, systematic supply, or distribution in any form to anyone is expressly forbidden.

The publisher does not give any warranty express or implied or make any representation that the contents will be complete or accurate or up to date. The accuracy of any instructions, formulae, and drug doses should be independently verified with primary sources. The publisher shall not be liable for any loss, actions, claims, proceedings, demand, or costs or damages whatsoever or howsoever caused arising directly or indirectly in connection with or arising out of the use of this material.

Measuring and Monitoring Optically Induced Thermal or Orientational Non-Locality in Nematic Liquid Crystal

Marc Warengthem

Jean François Blach

Jean François Henninot

Laboratoire de Physico-Chimie des interfaces et Applications,
LPCIA FRE CNRS, Université d'Artois, Lens cedex, France

Nonlinear propagation in nematic liquid crystals and spatial optical quasi-soliton can be generated via either thermal or orientational nonlinear process. These particular propagation modes can potentially be used in photonic and telecom devices, on the condition that they are well controlled, thus first to be properly measured. We first briefly review the measurements techniques, focussing on the newest one, based on a Raman scattering measurement. Then, it is demonstrated that there are two main ways to control the non-locality in spatial optical soliton either by using a time dependent source, or by playing with boundary conditions. Examples are given for each case.

Keywords: beam steering; nematic liquid crystals; nonlocality; optical soliton; Raman scattering

INTRODUCTION

Nonlinear optical phenomena in liquid crystal have been extensively studied after the pioneering works of N. Tabiryan and B. Zel'dovich [1]. Two non-local processes can cause "giant" nonlinear optical phenomena: thermal dependence of refractive indices and optical field sensitive alignment of the optical axis (Optical Freedericksz Effect, OFE), balanced by overall elastic boundary conditions. Amongst the possible phenomena, nonlinear propagation on long distance in nematic liquid crystals has been explored first [2], then studies have been focussed on spatial optical quasi-soliton. They can be generated

Address correspondence to Marc Warengthem, Laboratoire de Physico-Chimie des interfaces et Applications, LPCIA FRE CNRS 2485, Université d'Artois, SP18 62307 Lens cedex, France. E-mail: warengthem@univ-artois.fr

either via a thermal process [3] or an orientational one [4]. These particular propagation modes can potentially be used in photonic and telecom devices, on the condition that they are well controlled, which implies that non locality should be properly measured as well.

In this paper, non-locality refers to an effect that spreads beyond the cause. The processes involved in liquid crystal (LC) mentioned just above, which yield to the “giant” nonlinearity are of diffusive nature and are thus highly non-local. The thermal non linearity has been studied by F. Simoni and co-workers and reported in a book [5], however it deals with propagation in thin LC sample. Long haul propagation of thermally self focussed beams can be found in our papers. It is described the excitation of quasi soliton for the ordinary wave in the nematic phase and also the locally self induced phase transition, which allows light to be trapped in an isotropic tube it created [3,6]. Long haul propagation of orientationally self focussed beams has been first studied by E. Braun and co-workers [2,7]. Then, we have shown the possibility of using that to influence the defects in LC capillaries [8]. The possibility to excite a self waveguide or a quasi soliton exploiting the orientational non linearity has been demonstrated by G. Assanto and co-workers [4] and they pushed the study on both sides, theoretical and experimental, including the role of non-locality [9]. However, although quite comprehensive, the non locality issue is treated from the point of view of the resolution of propagation equation, the LC material and boundary conditions are more or less disregarded, although essential as it will be demonstrated in this paper. After these papers of the Roma group, other group reproduced quite similar experiments [10]. Recently, M. Karpierz and co-workers have shown the possibility to excite quasi soliton in a different geometry [11], which is an extra evidence of the fact that the optically induced reorientation is a perturbation in a graded index LC material, point which will be also considered herein. Apart these experimental works, it is worthy to notice the theoretical ones performed by W. Krolikowski et al. [12], which introduces, also from an optical point of view, the non-locality as a phenomenological parameter.

In this paper we would like to address the non-locality issue from the LC material point of view, including the boundary conditions. It contains mainly two parts, one devoted to the measurement of non locality and a second one devoted to its control. In the first part, it will be mainly reminded the measurement technique which allows the simultaneous measurements of both the optical field and the induced reorientation extensions in the case of a spatial soliton excited by orientational non-linearity. In the second part, the different possibilities to control the non-locality are analysed. It is shown that there are at least two main

ways to do it: either playing with a time dependent source (chopped source) or playing with boundary conditions. Obviously both ways can be used simultaneously. These two possibilities apply to both nonlinearities, thermal or reorientational. The four different cases are illustrated. Consequences of that approach are given and it is proposed a direct experimental evidence of the fact that for an optically induced reorientation, the director reorientation remains a local perturbation which does not relax across the LC. This has two consequences which are considered: first the non locality is determined by local boundary conditions, not by overall ones and second, as already observed by other researchers in the field, soliton behaves like a ray and launching a soliton in any index gradient allows performing experimental ray tracing.

Prior to enter the first part, let us briefly remind the way to excite a spatial soliton in LC. The clue is to balance the natural diffraction of a beam with a focussing effect, generated by the beam itself through a nonlinear effect. Whatever the nonlinearity involved, thermal or orientational, the geometry is the same, as depicted on the Figure 1: a beam is launched in a LC in such a way that it travels within the LC Material over a long distance. For a LC confined in a capillary, the beam is launched along with the capillary axis, and for a LC confined in a cell launched in a direction parallel to the walls of the cell.

In the case of the “thermal” soliton, the beam is partially absorbed by the LC and heats the medium: an initial gaussian beam is more intense in the central part of the beam than in its neighbour and thus the central part is hotter than its suburb. A temperature gradient is generated and providing that the temperature dependence of the index is large enough and with a positive dn/dT , the material becomes focussing. A small amount of dye will enhance the absorption and thus the

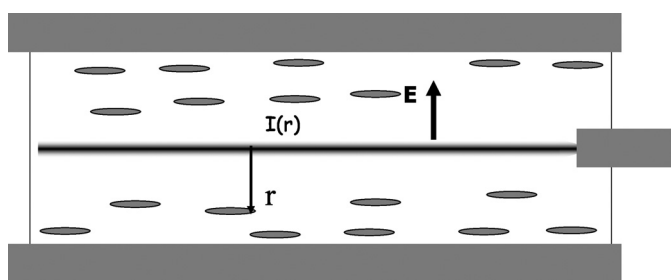


FIGURE 1 Overall geometry to excite a spatial soliton in nematic LC. The nonlinear action of the beam intensity distribution $I(r)$ generates an index distribution $n(T_{(r)})$ (“thermal” soliton) or $n(\theta_{(r)})$ (“orientational” soliton). The medium has to become focussing.

temperature gradient. Some nematic phases exhibit an ordinary index with a positive dn/dT . The soliton is obtained for the ordinary wave and in the case of a capillary geometry is polarisation independent.

In the case of the “orientational” soliton, the LC director is submitted to a torque proportional to the light intensity and which tends to align it towards the optical field. That torque is therefore stronger in the centre of the beam than in its suburb and as a result, the director alignment is different in the centre than in the suburb, generating a non-uniform director distribution and an index gradient for the extraordinary wave.

In both cases, the cause is the light intensity distribution $I(r)$ and the effect is the induced index distribution $n(T_{(r)})$ or $n(\theta_{(r)})$. Actually, strictly speaking this claim is not correct and that point is discussed in the second part, before let us first consider how these two distributions can be measured.

1. MEASUREMENT OF NON LOCALITY

The goal is to measure both distributions: beam intensity and induced index. There are several ways to measure the index distribution: interferometry and beam deflection are amongst those used. It has been proposed to insert the cell in a Mach Zehnder type interferometer [13,14], a fringe analysis allows retrieving the index distribution. However, that method just gives information on the index distribution, no direct information on the beam itself. Moreover, the fringe pattern being a phase shift integration across the cell, inversion to retrieve the original index distribution is all but an easy task, uniqueness of the solution might be questionable. The beam deflection measurement used to measure index gradient has been also proposed [15]. Considering that the involved gradients are quite small, the deflections are small as well and difficult to measure accurately: that technique is rather qualitative than quantitative one. However, contrarily to the previous one, it reveals the effect and views the cause. The measurement of the beam intensity distribution can be performed via an image analysis of the scattered light, which is also integrated across the cell thickness. We have recently proposed a new method to measure simultaneously both beam intensity and director distributions [16]. Since it will be called in the second part, we remind the essential feature of the technique.

The method consists in measuring the intensity of two Raman scattering modes excited by two sources. The principle is sketched on the Figure 2. The cell together with the fibre out of which the soliton is launched are placed on the stage of the micro Raman spectrometer

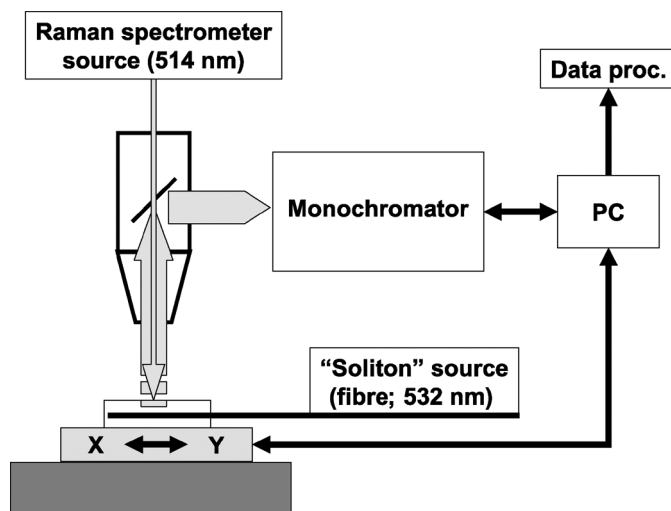


FIGURE 2 Geometry of the Raman scattering experiment. The sample is placed onto a x-y translation stage and on a microscope stage. Light scattered by the soliton beam and by the “source” beam is collected via the microscope and analysed via a monochromator.

set-up. The LC material scatters light coming from two sources. The first one is the laser beam attached to the Raman spectrometer, namely the Ar⁺ laser line at 514 nm (“Raman source”), which is focussed onto the cell through a microscope. The second excitation beam is the soliton itself, which is a laser beam at 532 nm, named “soliton source” in the following. Whole the scattered light is collected through the microscope objective and analysed via the monochromator. The recorded spectral range is selected on purpose to contain two peaks which can be unambiguously assigned. The first one from an highly polarised mode, associated with the “Raman source” reveals the director orientation (“orientation line” in the following). The second peak, not so strongly polarised and associated with the “soliton source,” reveals the soliton location and thus its extension (“soliton line” in the following). The used LC (E7 from Merck) contains cyanobiphenyls and the stretching mode of the triple bonds $C\equiv N$ is highly polarised with a Raman shift of 2224 cm^{-1} ; this will be the “orientation line.” The stretching mode of the $C-C$ in the aromatic rings are weakly polarised and has one out of its four Raman shifts at 1604 cm^{-1} (both herein announced shifts have been measured for our material) [17]. This peak is at 2243 cm^{-1} in the reference frame

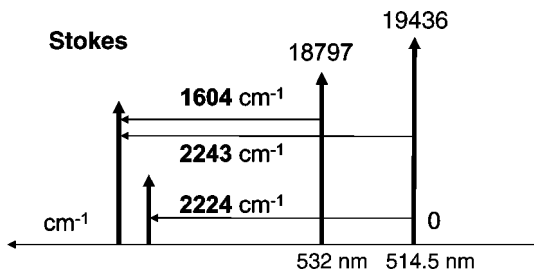


FIGURE 3 Relative position of the sources and peaks in the RAMAN monochromator reference frame.

of the spectrometer (514.5 nm; 19436.5 cm^{-1}), as shown on the Figure 3. Thus, the spectral range ($2100\text{--}2400\text{ cm}^{-1}$) contains the two unambiguously assigned peaks. The cell being installed on a translation stage as shown on the Figure 4, a x-y scanning is performed, set of spectra are collected for different positions of the cell with respect to the fixed Ar beam (Raman microscope). Considering a x-scan which crosses the soliton beam, the expected behaviour of the intensity of the two peaks is shown on the Figure 5. According to the Raman tensor of the stretching mode of the $\text{C}\equiv\text{N}$ bond and the geometry, the intensity of the “orientation line” is supposed to be maximum for a planar alignment and minimum for an homeotropic one. On the contrary, the intensity of the “soliton line” is maximum as the cell is placed in such a position that the soliton beam is just below the microscope and minimum (zero) as it is away from the microscope. Examples of experimental results can be found in the reference 16 and

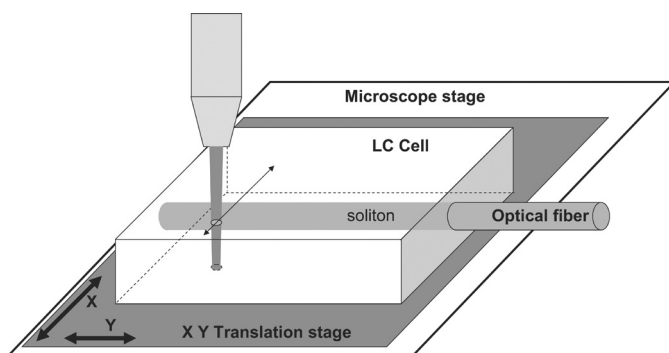


FIGURE 4 Reference frame and scanning geometry.

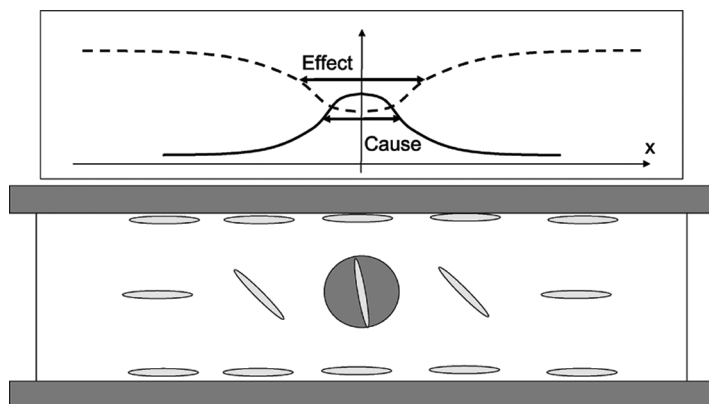


FIGURE 5 Cell geometry under study (bottom) and expected behaviour for both peaks (top). The ellipses figure the director, the grey circle the cross section of the soliton beam, travelling perpendicular to the plane of the drawing. On the top, the dashed line corresponds to the expected behaviour of the intensity of the $C\equiv N$ peak (2224 cm^{-1}) and the full line to the one of the $C-C$ peak (2244 cm^{-1}).

later on herein. Obviously the collected intensities are integrated across the cell thickness: improvement of this method by the use of immersion objective is underway, allowing a z-scan in addition to the x-y scan current capability.

2. MONITORING NON LOCALITY

In the introduction, it is mentioned that non locality refers to an effect that spread beyond the cause. In the herein studied systems – soliton like propagation in LC - the cause is the distribution of the laser beam intensity which turns to be collimated for some input power. The effect is the index gradient it creates (self wave guiding process). Strictly speaking, such a proposition is not correct: the cause cannot be restricted to the beam intensity distribution, it has to include the boundary conditions as well. The system can be described with two partial differential equations coupled by the index dependence on either the temperature or the director local alignment. The first equation rules the propagation (1) and the second the heat transfer in the case of a system driven by thermal non linearity (2) or the director alignment distribution (3), resulting from the minimisation of the elastic energy of the sample in the case of a system driven by OFE. These equations contain the different parameters characterising the physical system

(dielectric permittivity ε , heat conductivity Θ , absorption α , elastic constants K , viscosity γ) and it is beyond the scope of this paper to detail that aspect.

$$\Delta \cdot \vec{E} - \vec{\nabla}(\text{div}(\vec{E})) = -\mu_0 \cdot \omega^2 \cdot \vec{\varepsilon} \cdot \vec{E}; \text{div}(\vec{\varepsilon} \cdot \vec{E}) = 0 \quad (1)$$

$$\Delta T_{(r,z,t)} - \alpha \cdot |\mathbf{E}_{(r,z,t)}|^2 = \Theta \cdot \frac{\partial T_{(r,z,t)}}{\partial t} \quad (2)$$

$$K \cdot \Delta \theta_{(r,z,t)} + A \cdot |\mathbf{E}_{(r,z,t)}|^2 \cdot \sin(2\theta_{(r,z,t)}) = \gamma \frac{\partial \theta_{(r,z,t)}}{\partial t} \quad (3)$$

They are coupled via the electric field of the beam under study (cause) and via the dielectric permittivity tensor ε . The Eqs. (1) and (2) are coupled via the dependence on the temperature of the principal value ε_{\perp} , the expression of which being a characteristic of the LC material. The Eqs. (1) and (3) are coupled via the extraordinary index ($\sqrt{\varepsilon(\varepsilon_{\perp}, \varepsilon_{\parallel}, \theta)}$) seen by the wave which propagates. To these general equations, which have many possible solutions and thus many possible “non-locality,” we have to account for the boundary conditions which definitely select the physical solution for a given experimental system and thus ascribe a non-locality to a system. The main consequence of this affirmation is that the non-locality can be monitored via those boundary conditions. There is a second way to monitor the non-locality. It is a consequence of an observation we made several years ago and which is reported in the Ref. [18]. We tried to launch a soliton in a nematic material with a small birefringence (eutectic mixture of OS33 and OS53 from Merck, $\Delta n = 0.02$) and we only got a transient focusing behaviour, on the condition that the input intensity is increased fast enough. After a further analysis of the observed phenomenon [19], we arrived to the conclusion that at the onset of the intensity, the temporal derivative (rightmost term in Eqs. 2 and 3) are larger than the spatial derivatives (Laplacian in 2 and 3) and these latter can, to some extent, be neglected. Doing that, Eq. 2 reduces to:

$$\alpha \cdot |\mathbf{E}_{(r,z,t)}|^2 = -\Theta \cdot \frac{\partial T_{(r,z,t)}}{\partial t} \quad (4)$$

which is readily integrated and yields to an initial temperature distribution:

$$T_{(r,z)} = -\frac{\alpha}{\Theta} \cdot \int |\mathbf{E}_{(r,z,t)}|^2 \cdot dt \quad (5)$$

A similar treatment can be done to the Eq. 3. Equation (3) reduces to:

$$A \cdot |E_{(r,z,t)}|^2 \cdot \sin(2\theta_{(r,z,t)}) = \gamma \frac{\partial \theta_{(r,z,t)}}{\partial t} \quad (6)$$

adding the hypothesis of small reorientation, it becomes:

$$A \cdot |E_{(r,z,t)}|^2 \cdot 2\theta_{(r,z,t)} = \gamma \frac{\partial \theta_{(r,z,t)}}{\partial t} \quad (7)$$

which is readily integrated as well and yields to an initial director reorientation:

$$\text{Ln}(\theta_{(r,z)}) = \frac{A}{\gamma} \cdot \int |E_{(r,z,t)}|^2 \cdot dt \quad (8)$$

This explains why for our material with a small birefringence, the focussing occurs only transiently and for fast power increasing. This later experimental condition means a large time derivative of $E(r,z,t)$ in the equation and thus a large derivative dT/dt or $d\theta/dt$, and as a result, the distributions of temperature T or tilt angle θ given by (5) and (8) apply, they are similar to the intensity one. In other words, the director distribution orientation is as sharp as the beam itself, the index profile as well and the material is focussing, whatever the birefringence. However, the director distortion relaxes across the sample and the corresponding index profile is no longer sharp enough to guide the light, as the birefringence is small.

This approach can be turn in terms of non-locality: during the onset, the relationship (5) and (8) show that both distributions $T(r)$ and $\theta(r)$ are practically identical to the one of the beam intensity $E^2(r)$, which means that we are faced to a zero non-locality. The onset can be therefore considered as quasi local, whereas the steady state will be non-local. These two extreme cases (large time derivative and zero time derivative associated with local and non-local processes) open another possibility to monitor the non-locality: the use of time dependent source.

To summarise, non-locality can be monitored by playing either with boundary conditions and/or with the time dependence of the source, whatever the involved nonlinearity, thermal or orientational. We now report experimental examples of such monitoring for the different cases. Some have been already published and are just reminded (paragraph 2.1) some are new (paragraph 2.2).

2.1. Thermal Non-Linearity

This case of soliton excited by thermal nonlinearity has already been reported [3,6,8,15] and will be just reminded in order to put these experiments back in this monitored non-locality context.

2.1.a. Changing Boundary Conditions

In the case of a soliton excited via an index gradient obtained by a temperature gradient, the boundary conditions consist mathematically in imposing the temperature at the boundary together with the heat flux across the boundary. Physically, these conditions can be changed and selected by properly choosing the materials the system is made of. Any temperature control (Peltier type) can fix the external temperature and the heat capacity of the material fixes the flux. Thus, boundary materials impose the operating temperatures of the system and depending on the used LC, via its dn/dT , impose the range of index value that can be attained for a given input beam power. Apart these materials parameters, there is nothing else that can be used to monitor the non locality via boundary conditions. Possibilities offered by using chopped sources are more attractive.

2.1.b. Using Time Dependent Sources

This possibility has already been reported and exploited, yielding to curved self waveguide for instance. It will be therefore just reminded herein. In the specific case of 5CB (from Merck) doped with a slight amount of dye, two soliton like modes of propagation have been observed: one in the nematic phase and another in the isotropic phase. Actually, the energy absorbed by the dye and transformed in heat increases the temperature, and it can be done up to cross the clearing point (transition nematic to isotropic) which is around 35°C. The beam for input power large enough (around few mW, in our experiments) creates an isotropic tube in which the light is trapped. The length of the tube is reversibly correlated to the input power of the beam. Using a chopped source to excite the isotropic tube, it has been shown that its diameter depends on the pulse duration and its repetition rate. Out of this tube, a index gradient in the nematic phase is generated and by properly setting two isotropic tubes, a saddle like index gradient can be generated by the beams, light being trapped and guided in a curved waveguide [20].

2.2. Orientational Nonlinearity

In the case of orientational non-linearity, monitoring the non-locality using time dependent sources has already been recalled: our first

reported experiment shows a transient focussing in a nematic having a small birefringence. Experiments using materials with larger birefringence and chopped source are underway, a specific set-up being designed to measure this dynamic behaviour. The results will be reported in another paper. We herein focus on the soliton excited by optical reorientation and measuring the non-locality for different boundary conditions. We first checked experimentally that changing the boundary conditions actually changes the non-locality, then we report on the first direct experimental evidence of the fact that the optically induced reorientation is a perturbation that do not relax across the sample.

2.2.a. Changing Boundary Conditions

We prepared several cells as depicted on the Figure 6. The cell is made of ITO coated commercial glass plates, using fibre as spacers (125 μm diameter). Uniform LC planar alignment is achieved by conventional PVA coating, unidirectionally rubbed. The spacers are similarly treated. The anchoring energy is determined by the PVA rubbing performed using a brushing machine. Both glass plates and fibre spacers have been brushed the same way and anchoring energies are similar for each of the four walls limiting the LC. Brushing has been quite smooth, so our anchoring is supposed to be weak. Several cells have been prepared with the same brushing pressure, just changing the distance between the two spacers (d_s on the Figure 6). We measured the non-locality for these samples using the Raman based method reminded in the part 1. An example of results is shown on the Figure 7. Although it is beyond the scope of this paper to give a comprehensive study of the correlation between anchoring energies, geometry and reorientation width, a trend can be reported. For two samples with fibre distance equal to 10 and 6 mm we found a reorientation width of respectively 13 and 24 μm for a soliton beam

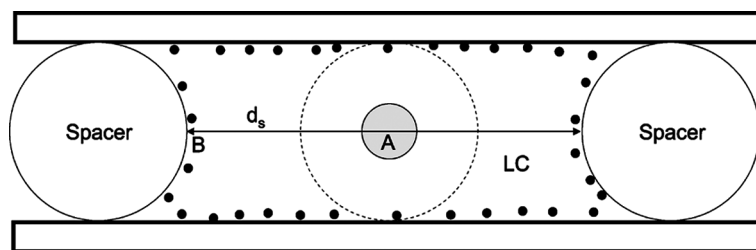


FIGURE 6 Cell geometry. Spacers are fibres. The grey circle stands for the cross section of the soliton beam.

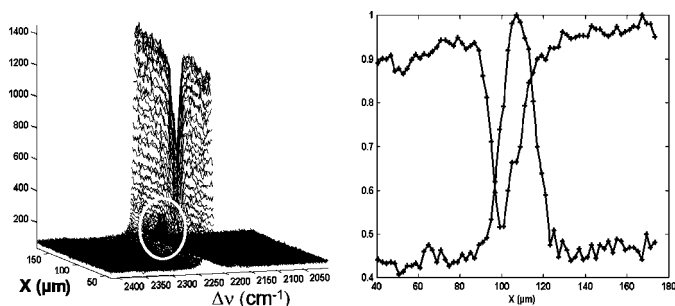


FIGURE 7 Example of Raman result. Left: collection of spectra for different x position of the sample. The line 2244 cm^{-1} is marked with a white circle. Right : plot of the maximum of both peaks versus x position of the cell. The behaviour looks like the one expected and shown on the Figure 5.

width of respectively 9 and $2\text{ }\mu\text{m}$. As the fibre distance is shortened, the reorientation radius decreases ($d_s = 300\text{ }\mu\text{m}$, reorientation width found to be $5\text{ }\mu\text{m}$). As it can be seen from these data, as the distance between spacers is large, there is no apparent correlation between widths of cause and effect (soliton beam radius and reorientation radius), on the contrary. This can be explained in considering the balance of walls and optical field torques: the closer they are to each other, the more they interact to yield to the steady director distribution. In the considered direction (ox, Figure 6), the shorter the distance between the spacer and the soliton, the stronger is their mutual influence. That distance has to be compared with the extrapolation length which is the ratio of the elastic constant over the anchoring energy. Typically this length is of the order of the micron for a strong anchoring and larger for weaker anchoring [21]. As already mentioned, this paper is devoted to show that playing with boundary conditions can help to monitor the non-locality, not to report on a comprehensive and quantitative study of the dependence of the non-locality on the anchoring energies and cell thickness. Such a study should account for the fact that it is a 3D torque balance and requires an experimental 3D mapping capability: this is underway.

While performing measurement of non-locality on cell with small d_s , we got direct experimental evidence that for small input beam power (large enough to excite soliton), the reorientation is a perturbation. We report on this specific result now.

2.2.b. Direct Experimental Evidence of Soliton as a “Stable” Perturbation

We prepared a cell as described in the previous paragraph, however, to enhance the effect we want to demonstrate, the two fibres spacers have been differently rubbed, so having different anchoring energies. Under the static electric field, applied to get rid of a threshold in the optical Freedericksz effect, the LC next to the fibre spacer having the lowest anchoring energy (A, Figure 6) will be more reoriented than the part in the other side (B, Figure 6). Using our Raman measurement method, the intensity of the “reorientation line” will be larger in the side A than in the side B. As the soliton is launched, the measurement of both Raman lines is performed and the obtained intensity for both lines is shown on the Figure 8. Contrarily to the example shown on the Figure 7, the hollow revealing the reorientation is practically not visible. However, if one subtracts the background (intensity recorded against x , while no soliton is launched) to this curve, one obtains a narrow hollowed curve, shown on the Figure 9. This reveals the optically induced reorientation, which is clearly a perturbation in a background index gradient (here induced by a specific boundary condition and static electric field). This result is consistent with observations made by experimentalists in the fields and raises a question. The question is: why this perturbation does not relax throughout the LC material? The answer is to be found in the overall torque balance: if one considers the surface, the static field and optical field torques balance, we expect that the surfaces do not intervene as long as the static field torque is larger than the surface one. The optical field torque balance the local static field torque. Thus the

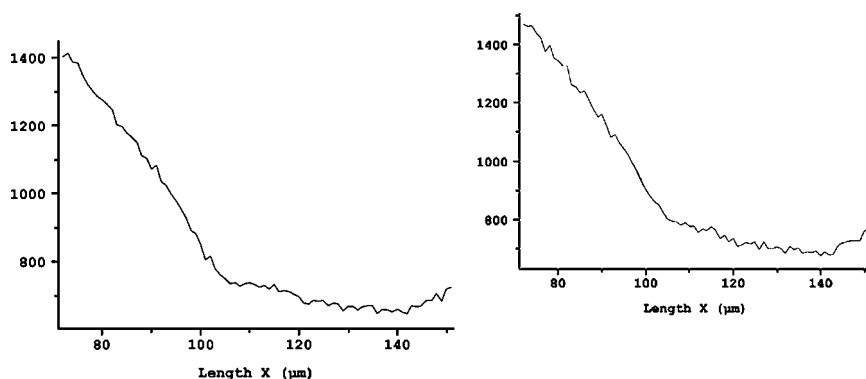


FIGURE 8 Intensity of the 2224 cm^{-1} peak versus x position of the cell, as the soliton beam is on.

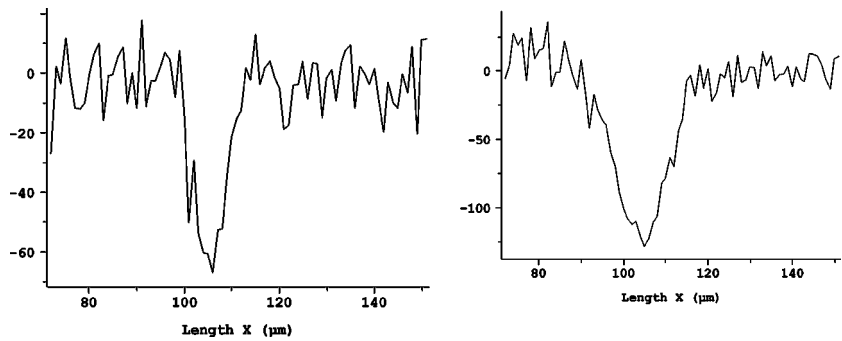


FIGURE 9 Same as on the Figure 8, the background (same peak with soliton beam off) has been subtracted. The dip due to the optically induced reorientation is clearly visible.

non-locality is fixed by this local balance and not by surfaces terms. This situation can be compared to a rubber ribbon glued on a table, pinned at both ends and which we want to strip off the table by pulling a needle underneath the ribbon (Fig. 10a). Depending on how strong is

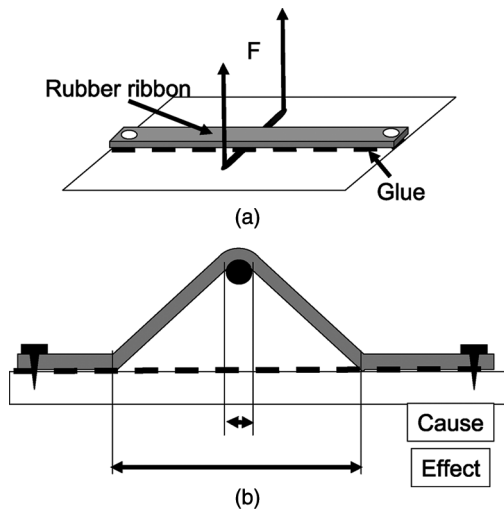


FIGURE 10 Analogy of the optically induced local reorientation with a rubber ribbon (LC), glued on a table (static electric field) and pinned at both side (anchoring energy), which we want to strip off the table by pulling a needle (optical field) (10a). For a light pulling force (optical field torque), the ribbon is strip off locally, whatever the pins (whatever the anchoring energy) (10b). The induced reorientation remains local and a perturbation.

the glue, a equilibrium is established, the ribbon is strip off only on some distance (Fig. 10b) which depends on the elasticity, the glue, not on the pins.

In badly aligned cell, we observed that it is possible to launch a soliton, however it is not propagating straight but is bent while crossing the defect region (similar result will be reported in the next paragraph): this is consistent with the fact that optically induced reorientation is just a local self created perturbation in the existing structure (index distribution). In other words, the soliton trajectory is equivalent to an experimental ray tracing. The observations reported in different geometry are similar [11,22]. An application of this is proposed in the next paragraph.

2.2.c. Application: Experimental Ray Tracing and Beam Steering

To illustrate the applicative potential of this result, we prepared a cell as previously described. The fibre spacer have been coated with PVA and rubbed the same way, to achieve equivalent anchoring energy on both sides, the width of the cell being around $250\mu\text{m}$. We managed to set a line defect (characteristic of the nematic phase) crossing the cell, as possible not perpendicular to the beam trajectory, in order to generate a director orientation gradient in the xz plane and as a result a beam deflection in that plane (Figs. 11a and b). Under a

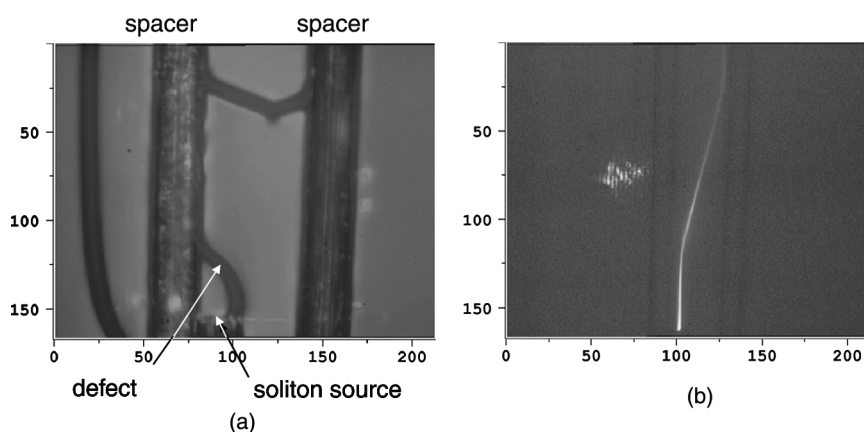


FIGURE 11 Photo of the cell prepared with two fibres as spacers and with a defect diagonally placed with respect to the soliton beam propagation which emerges out of the fibre marked as “soliton source” (11a). Propagation of a soliton through it (11b). Static voltage 1.6V.

quasi static applied voltage, the director field distribution changes, around the defect as well. A “orientational” soliton is then launched. Due to the director distribution around the defect, the soliton is propagating according to the associated index gradient as shown on the photo (Fig. 11). As the input beam power is kept constant and the bias voltage is increased, the director distribution changes and the “ray” follows up the index gradient, as shown on the Figure 12. The beam deviation is reversibly correlated to the director distribution thus to the applied voltage. A potential application in beam steering is obvious. For larger applied voltages, the input beam is no longer collimated: the optical torque (constant in this experiment) is no longer large enough to overcome the torque due to the applied voltage and the induced waveguide can not be created.

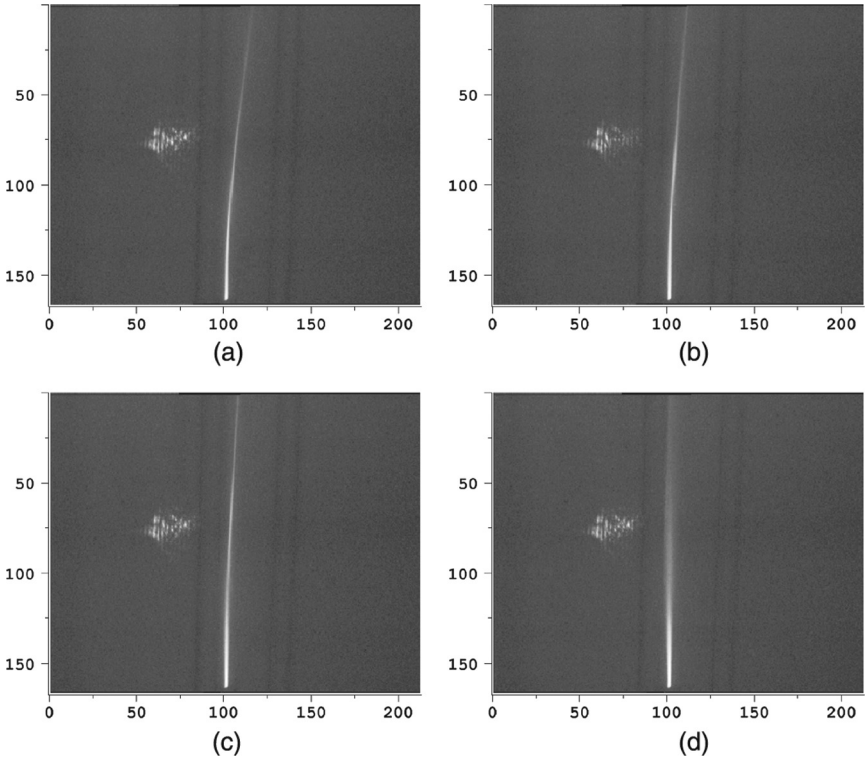


FIGURE 12 Same as photo 11b with different static voltages. Clockwise from top left: 12a $V = 2.1$ V; 12b $V = 2.5$ V; 12c $V = 3$ V; 12d $V = 5$ V. In this latter case, the beam is no longer collimated, the optical torque being too weak to induced a waveguide.

CONCLUSION

We have considered the propagation of a laser beam in a nematic liquid crystal material and its possibility to self-collimate (soliton like propagation) either via a thermal process or an orientational one. The role of non-locality is considered in order to control the resulting propagation. From the equations that rule the processes, it is deduced that there are at least two ways to control the overall propagation process (induced index gradient): it can be done either by adjusting the boundary conditions or by injecting a chopped source, adjusting the repetition rate and pulse length. This is valid for both non-linearity, thermal or orientational. For soliton launched using the orientational process, it is demonstrated for the first time experimentally that the beam generates a local perturbation which do not relax across the nematic cell, the “self wave-guide.” This result raise two points: first the non-locality is determined by an overall torque balance and not only by strict boundary conditions and second, the soliton like propagation behaves like an experimental ray tracing. An immediate consequence is the possibility to use that last point in beam steering device: soliton beam can be driven in any index structure which can be monitored via any external action. Demonstration of collimated beam deflection is proposed using a simple defect monitored via a bias voltage.

REFERENCES

- [1] Tabiryan, N. V. & Ya Zel'dovich, B. (1981). *Mol. Cryst. Liq. Cryst.*, 62, 637.
- [2] Braun, E., Faucheux, L., & Libchaber, A. (1993). *Phys. Rev. A*, 48/1, 611.
- [3] Warengthem, M., Henninot, J. F., & Abbate, G. (1998). *Opt. Exp.*, 2, 483.
- [4] Peccianti, M., de Rossi, A., Assanto, G., de Luca, A., Umeton, C., & Khoo, I. C. (2000). *Appl. Phys. Lett.*, 77, 7.
- [5] Simoni, F. (1997). *Nonlinear Optical Properties of Liquid Crystals and PDLC, Series on Liquid Crystals*, Chap. 4, World Scientific: Singapore, Vol. 2, 143.
- [6] Henninot, J. F., Debailleul, M., Derrien, F., & Warengthem, M. (2003). *J. Opt. A: Pure Appl. Opt.*, 5, 250.
- [7] Braun, E., Faucheux, L., Libchaber, A., McLaughlin, D. W., Muraki, D. J., & Shelley, M. J. (1993). *Europhys. Lett.*, 23(4), 239.
- [8] Warengthem, M., Henninot, J. F., & Abbate, G. (1998). *Mol. Cryst. Liq. Cryst.*, 320, 207.
- [9] Conti, C., Peccianti, M., & Gaetano, G. (2003). *Phys. Rev. Lett.*, 91(7), 073901.
- [10] Beeckman, J., Neyts, K., Hutsebaut, X., Cambournac, C., & Haelterman, M. (2004). *Opt. Exp.*, 12(6), 1011.
- [11] Brzdakiewicz, K. A., Sierakowski, M. W., & Karpierz, M. A. (2005). *Proceeding SPIE*, 5949–15.
- [12] Krolikowski, W., Bang, O., Nikolov, N. I., Neshev, D., & Wyller, J. (2004). *J. Opt. B*, 6, S288.

- [13] Hutsebaut, X., Cambournac, C., Haelterman, M., Beeckman, J., & Neyts, K. (2004). Nonlinear guided waves and their applications, Technical digest, Toronto, 28–31 March.
- [14] Henninot, J.-F., Derrien, F., & Warenghem, M. (2002). International workshop on bulk surface effects in liquid crystals for photonic applications, St Margerita di Pula, 15–21 October, Cagliari, Sardinia, Italy.
- [15] Henninot, J. F., Debailleul, M., & Warenghem, M. (2002). *Mol. Cryst. Liq. Cryst.*, 375, 631.
- [16] Warenghem, M., Henninot, J. F., & Blach, J. F. Proceedings SPIE, 5947–27.
- [17] Gray, G. W. & Mosley, A. (1976). *Mol. Cryst. Liq. Cryst.*, 35, 71–81.
- [18] Warenghem, M., Henninot, J. F., & Abbate, G. (1999). *J. of Nonlinear Optical Phys. & Materials*, 8(3), 341.
- [19] Santamato, E. (1999). Private communication.
- [20] Henninot, J. F., Debailleul, M., Asquini, R., d'Alessandro, A., & Warenghem, M. (2004). *J. Opt. A: Pure Appl. Opt.*, 6, 315.
- [21] See for instance Faetti, S. (1991). *Physics of Liquid Crystalline Materials*, Chap. 12, Gordon & Breach: Paris, 301.
- [22] Peccianti, M., Fratalocchi, A., & Gaetano, G. (2004). *Opt. Exp.*, 12, 6524.